

Comparative Study of Different Vehicle Models with Respect to Their Dynamic Behaviour

G. Papaioannou*, A. M. Dineff and D. Koulocheris

Vehicles Laboratory, School of Mechanical Engineering
National Technical University of Athens,
Zografou Campus, Iroon Polytechniou 9, Athens, 15780, Greece
*Email: gpapaioan@central.ntua.gr

ABSTRACT

Various simulation models are used extensively for the design and the optimisation of vehicle suspension systems, as well as the application of various control algorithms in them. The selection of the most suitable model for these purposes is never explained and many times unnecessary complexity is added in them. In this respect, an assessment regarding the accuracy of the most common vehicle models is conducted. Thus, four vehicle models with various configurations are compared in terms of accuracy. More specifically, both passive and semi active suspensions are employed to the models, while the effect of adding anti-roll bars and tire dampers is also investigated. The transient behaviour of the suspension system and the overall vehicle performance are assessed in terms of ride comfort, vehicle handling and road holding using different road excitations. The results illustrate the ability of lower accuracy models to cope well and that they should be preferred most of the times. Also, anti-roll bars and tire dampers should be neglected when the ride comfort is investigated, whereas they have to be included when simulations regarding road holding are conducted.

Keywords: vehicle dynamics; simulation models; transient; dynamic; comfort; holding.

INTRODUCTION

Multibody dynamics and rigid bodies have been used extensively by the automotive industry so as to model and design the vehicle and its parts. In order to investigate the behaviour of a vehicle, the discrete modelling employing lumped masses is usually used. A lumped mass model is a simplified representation of the vehicle, where the suspension system is assumed to act as a single lumped mass which can only translate in the vertical direction with respect to the vehicle body. This mass is connected to the vehicle body at the wheel centre with a translational joint, allowing only the vertical motion.

Depending on the focus of each study, various models have been used in order to simulate the dynamic behaviour of a vehicle by modelling the tires, the body and the suspension system. Simple models of one or two degrees of freedom (quarter car model [1–3]), can be found in the literature. Since the quarter car model does not take into account any rotational degrees of freedom, its usage is limited to fairly simple suspension design optimisation problems and preliminary results. For more accurate results, though, models of a higher level of complexity should be used. Koulocheris et al. [4] used a half-car model with degrees of freedoms the vertical displacement and the roll angle of the sprung mass and the displacements of the rear right and left unsprung masses comparing the results of the simulation with tire forces evaluated experimentally. Similar half-car

model was used also by Papaioannou et al. [5, 6] and Koulocheris et al. [7, 8] including the pitch angle instead of in the dynamic behaviour of the vehicle. Full car models are the most complex ones with seven or eight degrees of freedom offering the most accurate simulation. Despite being time-consuming, they are widely used in research such as the works of Fossati et al. [9] optimised it in terms of ride comfort and vehicle stability and Abdelkareem et al. [10]. Seifi et al. [11] used a full car ride model along with a full car lateral model to study the rollover dynamics of a vehicle. In addition, more detailed models have been developed studying the lateral dynamics of the vehicle simultaneously with the vertical ones, such as the work of Shim et al. [12], Tchama et al. [13] and Cao et al. [14]. Although, the need for knowing many vehicle parameters is an important disadvantage along with the fact that they are the most time consuming of all.

However, the selection of the most suitable model for suspension design is never explained and many times unnecessary complexity is added, either by using a model with more degrees of freedom or by adding more elements in the one selected (anti-roll bars, tire dampers etc.). The decision regarding the most appropriate model doesn't depend only on the fact that the pitch phenomena or the roll phenomena, should be investigated. The suspension design engineers in Research and Industry have to consider if the increase in the DoFs of the model or the elements included will provide more accurate results and the computational time demanded will worth it. Thus, the decision has to be made based on the intended application, i.e. road excitation, the reason of simulations (ride comfort or road holding), optimisation of the suspension etc. without neglecting the complexity and the computational time.

Based on the above, the aim of this paper is to conduct an assessment regarding the accuracy of the four most common vehicle models. In contrast to Faris et al. [15] and Ihsan et al. [16, 17] who conducted comparative works more with respect to different semi-active control algorithms than with respect to vehicle models, in this work, the vehicle models with various configurations are compared in terms of accuracy and with respect to different performance metrics. More specifically, both passive and semi-active suspensions are considered, while the effect of adding anti-roll bars and tire dampers is also investigated. The transient behaviour of the suspension system and the overall ride performance of the vehicle are assessed in terms of ride comfort and road holding using different road excitations. Important conclusions are derived regarding their accuracy.

The organization of the paper is as follows: firstly, a description of all the vehicle models and their performance metrics are presented, then the road excitation applied to them are illustrated, while in the next chapter the case studies are displayed and their results are discussed extensively, finally conclusion is excluded.

SIMULATION MODELS

Various lumped masses models have been developed using the rigid body mass theory, considering the following [18].

- i. The tires are always in contact with the ground, which is true at low frequency but might not be true at high frequency. Also, the camber angle between the wheels and the body is considered constant.
- ii. The aerodynamic forces, as well as the rolling resistance of the tires, are neglected.
- iii. The centre of gravity of the vehicle is assumed to be above the roll and pitch centres.
- iv. The deflections in the roll and pitch planes are small enough to use the approximate theory for small angles.

The main vehicle models existing in the literature are the quarter car (QC), the half-car, either considering the front and rear axle (HC2) or the right and the left wheel of one axle (HC1), and the full car (FC). All of them consider four basic subsystems: the sprung mass, the unsprung masses and the corresponding suspension systems, and the tires. Their suspension systems, as well as the tires, are modelled as springs and dampers and the irregularities of the road profile are applied as inputs to the models through the tires. Simulating these models, important aspects of vehicle dynamics and suspension's performance can be evaluated. First of all, the suspension performance is assessed through its transient and steady-state response. Furthermore, the vehicle performance is studied by evaluating the ride comfort of the passengers and the vehicle's handling and road holding.

Quarter Car Model (QC)

The quarter car model is considered as a rigid body of mass $m_{1/4}$, equal to the one-quarter of the total mass of the vehicle ($m_{1/4}=m_s/4$). It represents any of the four suspension systems of the vehicle and its degrees of freedom (DOFs) are the displacement of the sprung mass ($z_s - m_s$) and of the unsprung mass ($z_u - m_u$). The effects of the coupled masses are neglected in this model. The governing equations of the QC vehicle model occur from its free body diagram (Figure 1) are given by Eq. (1) and (2). The nomenclature of the parameters included in the equations is presented in Table 1.

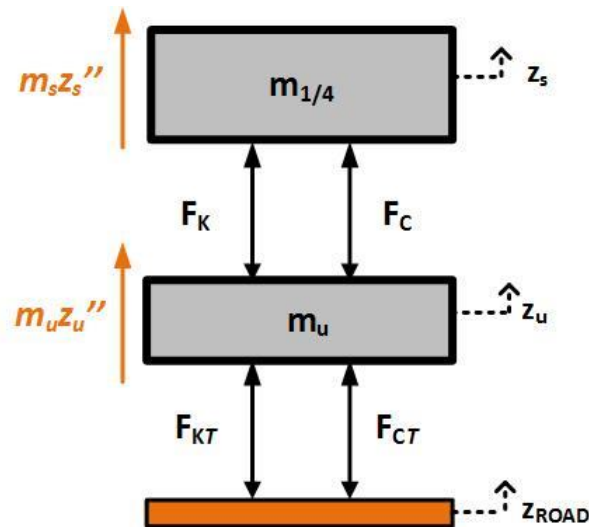


Figure 1. Quarter Car.

$$\text{Body bounce: } m_{1/4}\ddot{z}_s + F_C + F_K = 0 \quad (1)$$

$$\text{Wheel bounce: } m_u\ddot{z}_u - F_C - F_K + F_{CT} + F_{KT} = 0 \quad (2)$$

where F_K and F_C correspond to the forces applied by the suspension spring and damper respectively and depend on the suspension travel and its velocity, while F_{KT} and F_{CT} correspond to the forces applied by the tire spring and damper respectively and are related with the tire deflection and its velocity.

Table 1. Nomenclature of parameters of the vehicle model.

| Parameters | Description | Subscripts | Description |
|---------------------------|--------------------------------|------------|---------------|
| z (m) | vertical displacement | s | sprung mass |
| φ (rad) | roll angle | u | unsprung mass |
| θ (rad) | pitch angle | T | tire |
| Z_{road} (m) | road excitation | K | spring |
| F (N) | force | C | damper |
| M (Nm) | moment | KT | tire spring |
| m (kg) | mass | CT | tire damper |
| k (N/m) | spring stiffness | x | x-axis |
| c (Ns/m) | damping coefficient | y | y-axis |
| I_x (kgm ²) | longitudinal moment of inertia | F | front axle |
| I_y (kgm ²) | lateral moment of inertia | R | rear axle |
| b (m) | distance from CG to each side | 1 | right wheel |
| a (m) | distance from CG to each axle | 2 | left wheel |
| w (m) | wheelbase ($=a_F+a_R$) | AR | anti-roll bar |

Half Car Model (HC1)

In order to study the roll vibrations of a vehicle, the half-car model (HC1) is used and is shown in Figure 2. This model considers the right and left wheel of one of the vehicle's axles. The body of the vehicle is considered as a rigid mass $m_{1/2}$, equal to the half of the total mass of the vehicle ($m_{1/2}=m_s/2$), with a longitudinal moment of inertia I_{xx} , equal to the half of the total body mass moment ($I_{xx}=I_v/2$). Additionally, this model may also include an anti-roll bar with torsional stiffness k_{AR} , which provides a torque M_{AR} proportional to the roll angle φ as in Eq. (7). The degrees of freedom (DOFs) of the model are the roll and heave motions of the sprung and unsprung masses. The governing equations of the model are presented in the following differential equations Eq. (3) to (6).

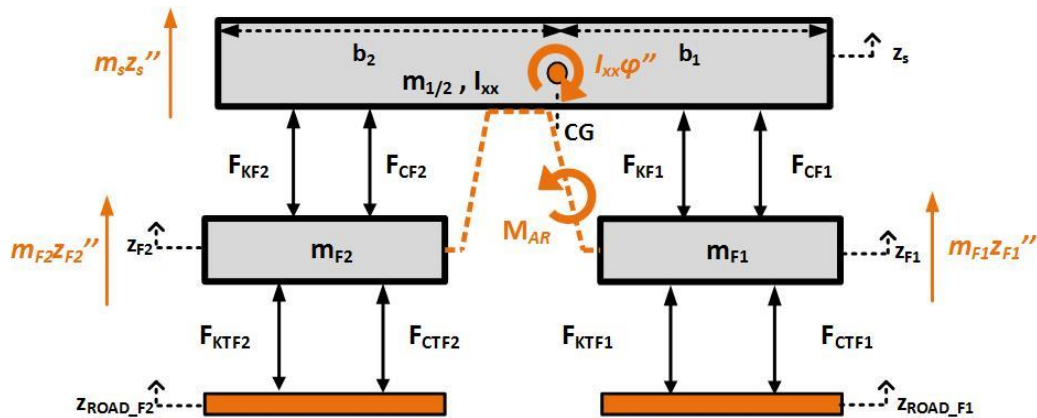


Figure 2. Half-car model (HC1).

$$\text{Body Bounce: } m_{1/2}\ddot{z}_s + F_{CF1} + F_{CF2} + F_{KF1} + F_{KF2} = 0 \quad (3)$$

$$\text{Roll Bounce: } I_{xx}\ddot{\varphi} + b_1F_{CF1} - b_2F_{CF2} + b_1F_{KF1} - b_2F_{KF2} + M_{AR} = 0 \quad (4)$$

$$\text{Right Wheel Bounce: } m_{F1}\ddot{z}_{F1} - F_{CF1} - F_{KF1} + F_{CTF1} + F_{KTF1} + F_{AR} = 0 \quad (5)$$

$$\text{Left Wheel Bounce: } m_{F2}\ddot{z}_{F2} - F_{CF2} - F_{KF2} + F_{CTF2} + F_{KTF2} - F_{AR} = 0 \quad (6)$$

where F_{Ki} and F_{Ci} correspond to the forces applied by the spring and the damper of the i^{th} suspension systems ($i=F1, F2, R1$ and $R2$) and depend on the suspension travel and its velocity, while F_{KTi} and F_{CTi} correspond to the forces applied by the spring and damper of i^{th} tire ($i=F1, F2, R1$ and $R2$) and depend on the tire deflection and its velocity. As far as the anti-roll bar is concerned, the torque it provides is calculated according to the Eq. (7), while the force that the anti-roll bar applies to the wheels is given by the Eq. (8).

$$M_{AR} = -k_{AR}\varphi \quad (7)$$

$$F_{AR} = M_{AR}/w \quad (8)$$

Half Car Model (HC2)

Another version of the half-car model considers the front and the rear axle of the vehicle. It is illustrated in Figure 3 and it is used to investigate the pitch vibrations of the vehicle. It considers the body of the vehicle as a rigid mass $m_{1/2}$, equal to the half of the total mass of the vehicle ($m_{1/2} = m_s/2$), and lateral moment of inertia I_{yy} , which is the half of the total body's lateral moment of inertia ($I_{yy} = I_y/2$). The DOFs are the pitch and bounce motions of the sprung and unsprung masses. The governing equations of motion for this model are given by the following Eq. (9) to (12).

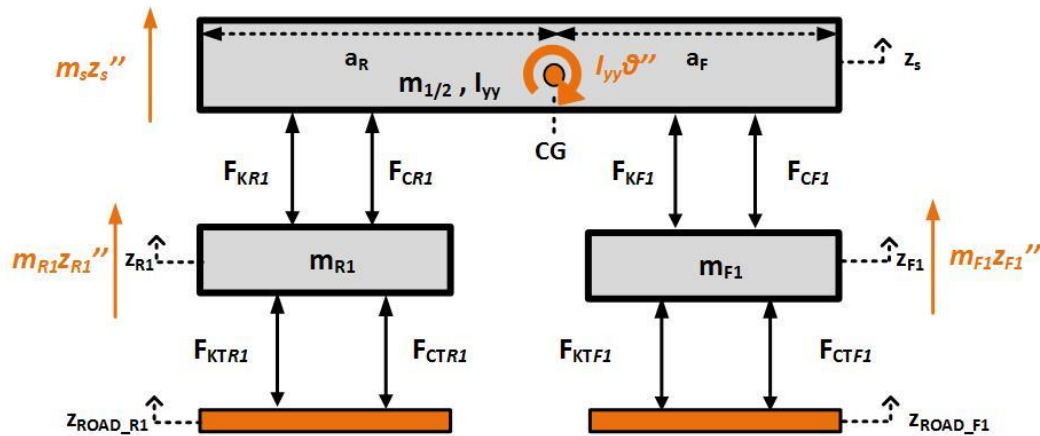


Figure 3. Half Car Model (HC2).

$$\text{Body Bounce: } m_{1/2}\ddot{z}_s + F_{CF1} + F_{CR1} + F_{KF1} + F_{KR1} = 0 \quad (9)$$

$$\text{Pitch Bounce: } I_{yy}\ddot{\theta} - a_F F_{CF1} + a_R F_{CR1} - a_F F_{KF1} + a_R F_{KR1} = 0 \quad (10)$$

$$\text{Front Wheel Bounce: } m_{F1}\ddot{z}_{F1} - F_{CF1} - F_{KF1} + F_{CTF1} + F_{KTF1} = 0 \quad (11)$$

$$\text{Rear Wheel Bounce: } m_{R1}\ddot{z}_{R1} - F_{CR1} - F_{KR1} + F_{CTR1} + F_{KTR1} = 0 \quad (12)$$

where F_{Ki} and F_{Ci} correspond to the forces applied by the spring and the damper of the i^{th} suspension systems ($i=F1, F2, R1$ and $R2$) and depend on the suspension travel and its velocity, while F_{KTi} and F_{CTi} correspond to the forces applied by the spring and damper of i^{th} tire ($i=F1, F2, R1$ and $R2$) and depend on the tire deflection and its velocity.

Full Car Model (FC)

The most detailed vibrating model of a vehicle is the so-called full car model (FC), as illustrated in Figure 4. This model is of seven degrees of freedom (DOFs) including the roll (φ) and the pitch angle (θ) of the sprung mass, as well as the heave motions of the vehicle body (z_s) and of the vehicle's wheels (z_{F1}, z_{F2}, z_{R1} and z_{R2}). The current model considers the vehicle body as a rigid mass m_s , equal to the total mass of the vehicle, with a longitudinal and lateral moment of inertia I_x and I_y , respectively. Additionally, an anti-roll bar with torsional stiffness k_{ARi} providing torque M_{ARi} for front ($i=F$) and rear ($i=R$) axle can also be considered. The governing equations of FC model occur from its free body diagram, as presented in Figure 4 and Eq. (13) to (19), while the nomenclature of the parameters included in the equations is presented in Table 1.

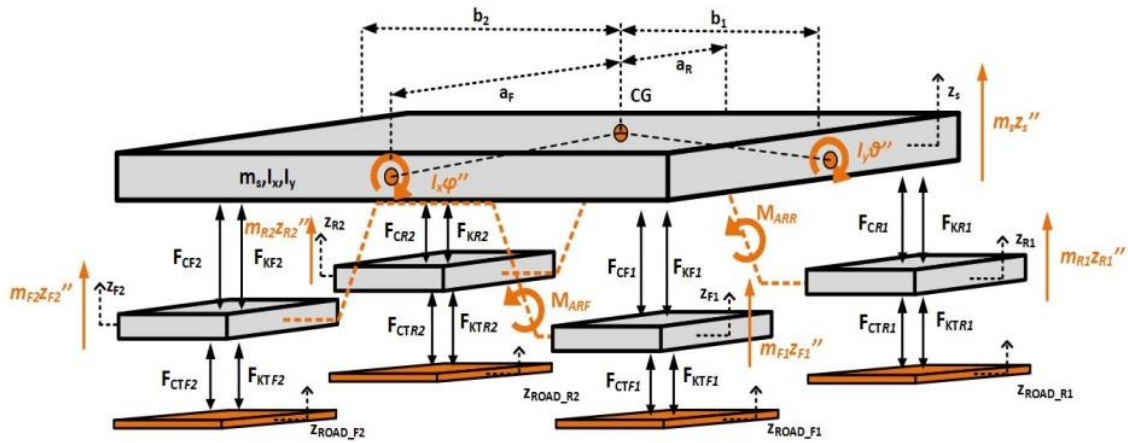


Figure 4. Full Car Model (FC).

$$\text{Body Bounce: } m_s \ddot{z}_s + F_{CF1} + F_{CF2} + F_{CR1} + F_{CR2} + F_{KF1} + F_{KF2} + F_{KR1} + F_{KR2} = 0 \quad (13)$$

$$\text{Roll Bounce: } I_x \ddot{\varphi} + b_1 F_{CF1} - b_2 F_{CF2} + b_1 F_{CR1} - b_2 F_{CR2} + b_1 F_{KF1} - b_2 F_{KF2} + b_1 F_{KR1} - b_2 F_{KR2} + M_{ARF} + M_{ARR} = 0 \quad (14)$$

$$\text{Pitch Bounce: } I_y \ddot{\theta} - a_F F_{CF1} - a_F F_{CF2} + a_R F_{CR1} + a_R F_{CR2} - a_F F_{KF1} - a_F F_{KF2} + a_R F_{KR1} + a_R F_{KR2} = 0 \quad (15)$$

$$\text{Front Right Wheel Bounce: } m_{F1} \ddot{z}_{F1} - F_{CF1} - F_{KF1} + F_{CTF1} + F_{KTF1} + F_{ARF} = 0 \quad (16)$$

$$\text{Front Left Wheel Bounce: } m_{F2} \ddot{z}_{F2} - F_{CF2} - F_{KF2} + F_{CTF2} + F_{KTF2} - F_{ARF} = 0 \quad (17)$$

$$\text{Rear Right Wheel Bounce: } m_{R1} \ddot{z}_{R1} - F_{CR1} - F_{KR1} + F_{CTR1} + F_{KTR1} + F_{ARR} = 0 \quad (18)$$

$$\text{Rear Left Wheel Bounce: } m_{R2} \ddot{z}_{R2} - F_{CR2} - F_{KR2} + F_{CTR2} + F_{KTR2} - F_{ARR} = 0 \quad (19)$$

where F_{Ki} and F_{Ci} correspond to the forces applied by the spring and the damper of the i^{th} suspension systems ($i=F1, F2, R1$ and $R2$) and depend on the suspension travel and its velocity, while F_{KTi} and F_{CTi} correspond to the forces applied by the spring and damper of i^{th} tire ($i=F1, F2, R1$ and $R2$) and depend on the tire deflection and its velocity.

Forces and Moments of the Simulation Models

The force by the suspension spring occurs ($F_{Ki}=k_iST_i$) by multiplying the spring constant (k_i) with the suspension travel (ST_i) for each wheel ($i= \emptyset, F1, F2, R1, R2$), as presented in Eq. (20) for the QC, HC1, HC2 and FC models, respectively. Also, the force due to the tire spring occurs ($F_{KTi}=k_{Ti}TD_i$) by multiplying the tire spring coefficient (k_T) with the tire deflection (TD_i). The suspension travel (ST_i) and the tire deflection (TD_i) are given by the Eq. (20) and (21), respectively, as evaluated using the FC model. In case of the half car models, the ST and the TD are decreased to two equations (F1 and F2 or F1 and R1 for HC2 and HC1 respectively) based on the suspensions systems number and they occur by setting as zero a_F and a_R or b_1 and b_2 for HC2 and HC1, respectively. Moreover, for QC, one ST and one TD occur by setting as zero all the above.

$$ST_i = \begin{cases} z_s - z_{F1} + b_1\varphi - a_F\theta, & i=F1 \\ z_s - z_{F2} - b_2\varphi - a_F\theta, & i=F2 \\ z_s - z_{R1} + b_1\varphi + a_R\theta, & i=R1 \\ z_s - z_{R2} - b_2\varphi + a_R\theta, & i=R2 \end{cases} \quad (20)$$

$$TD_i = \begin{cases} z_{F1} - z_{road_{F1}}, & i=F1 \\ z_{F2} - z_{road_{F2}}, & i=F2 \\ z_{R1} - z_{road_{R1}}, & i=R1 \\ z_{R2} - z_{road_{R2}}, & i=R2 \end{cases} \quad (21)$$

In addition, the force applied due to the suspension damper occurs ($F_{Ci}=c_i\dot{ST}_i$) by multiplying the viscous damping coefficient (c_i) with the suspension travel velocity (\dot{ST}_i) for each wheel ($i= \emptyset, F1, F2, R1, R2$). As far as the passive dampers are concerned, they are considered to operate with a constant coefficient. In this work, we also investigate the accuracy of the models with semi-active suspensions. Thus, the models presented before (QC, HC1, HC2, FC) are employed with semi-active suspension systems operating with the SH-2 states control law. This particular control is an on-off strategy consisting of two states in which the damping factor (c_i) switches between soft and stiff damping coefficients according to the sign of the product of the sprung mass velocity (\dot{z}_s) and the suspension travel velocity (\dot{ST}_i). In this case, the equation describing the control algorithm is presented in Eq. (22).

$$c_i = \begin{cases} c_{min}, & \text{if } \dot{z}_s \dot{ST}_i \leq 0 \\ c_{max}, & \text{otherwise} \end{cases} \quad (22)$$

where $i= \emptyset, F1, F2, R1, R2$, and c_{min} and c_{max} are the minimum and maximum damping factors achievable by the considered controlled damper, depicting the soft and firm damping coefficient respectively. As far as the force by the tire damper ($F_{CTi}=c_{Ti}\dot{TD}_i$) is

concerned, it is calculated as the product of the tire damping coefficient (c_{Ti}) and the tire deflection velocity ($T\dot{D}_i$).

Performance Metrics

The main aim of this work is to compare the accuracy of the mathematical models regarding various aspects of vehicle performance. For this reason, we focus both on the transient behaviour of the suspension and the overall vehicle performance. The latter is related not only to ride comfort but also to the vehicle handling and road holding. In this section, all of these aspects are investigated and quantified.

Transient response

Systems like vehicles, which include energy storage, cannot respond instantaneously when they are subjected to disturbances and thus, they exhibit transient responses. The transient response depends on the initial conditions of the system and for comparing them, it is common to consider that the vehicle is initially at rest and all the time derivatives, therefore, are zero. In order to specify the transient response characteristics, it is common to use the following metrics:

- i. Peak time (t_p) is the time required for the response to reach the first peak of the overshoot and it displays the responsiveness of the system.
- ii. Peak (M_p) is the maximum value of the response curve and corresponds to peak time.
- iii. Settling time (t_s) is defined as the time required for the system in order for the response to reach and stay within $\delta\%$ range of the steady-state value. The settling time is related to the largest time constant of the system.

In vehicle dynamics, transient response is investigated for assessing the suspension performance, since vehicles are mostly time-domain systems, and they have to exhibit acceptable time responses. Therefore, the time-domain metrics presented above are quite important. Except for certain applications where oscillations cannot be tolerated, it is desirable that the transient response be sufficiently responsive and damped.

Ride comfort

In order to ensure good ride quality, the suspension system should be able to isolate the car body from road disturbances by reducing the vibratory forces transmitted from the axle to the vehicle body, and thus the vehicle body acceleration. Since the vehicle model doesn't consider a seat model or a passenger model, the ride comfort can be quantified by the measurements of the vertical acceleration of the sprung mass (\ddot{z}_s). More specifically, the ride comfort could be measured via the weighted root mean square (RMS) of the acceleration (\ddot{z}). This characteristic is proposed by the ISO-2631 regulation which evaluates the human exposure to whole-body vibration [19]. More specifically, the weighted RMS acceleration is calculated as follows:

$$RC = RMS(\ddot{z}_{wi}) = \sqrt{\frac{1}{T} \left(\int_0^T \ddot{z}_{wi}(t)^2 dt \right)} \quad (23)$$

where T is the duration of the measurement in seconds, \ddot{z}_{wi} is the weighted acceleration as a function of time (m/s^2) and i is the selected subsystem of the driver or the vehicle model. In this work, where no seat model or passenger model are used, we consider the acceleration of the sprung mass, thus $i=s$.

Road holding and handling

Important metrics indicating the dynamic behaviour of the vehicle are the suspension travel and the tire deflection. The suspension travel depicts the ability of the suspension system to support the static weight of the vehicle. If the rattle space requirements of the vehicle are kept small, then the vehicle's static weight is well supported. The tire deflection of the system and thus the normal tire forces demonstrate the vehicle handling and road holding. This performance can be characterized in terms of vehicle's cornering, braking and traction abilities. These abilities can be improved by minimising the variations in normal tire loads, due to the fact that the lateral and the longitudinal forces generated by a tire depend directly on the normal tire load. So, considering that a tire roughly behaves like a spring in response to vertical forces, the variations in normal tire load can be directly related to the vertical tire deflection. Thus, the maximum values as well as the variances of these quantities could be a good index for vehicle's suspension system behaviour as well as the road holding and handling. The maximum value and the variance of the suspension travel are given by Eq. (24) and (25), respectively.

$$MST_i = \max(ST_i) \tag{24}$$

$$VST_i = \frac{1}{n-1} \sum_{j=1}^n |ST_{i,j} - \overline{ST}_i|^2 \tag{25}$$

where j corresponds to an element of the suspension travel's dataset, n is the number of elements of the dataset and $i = \emptyset, F1, F2, R1, R2$. The maximum value and the variance of the suspension travel are calculated as in Eq. (26) and (27).

$$MTD_i = \max(TD_i) \tag{26}$$

$$VTD_i = \frac{1}{n-1} \sum_{j=1}^n |TD_{i,j} - \overline{TD}_i|^2 \tag{27}$$

where j corresponds to an element of the tire deflection's dataset, n is the number of elements of the dataset and $i = \emptyset, F1, F2, R1, R2$.

EXCITATION

The irregularities on the road cause disturbances and are classified as shock or vibration. The first is related to discrete disturbances, usually associated with higher amplitudes, such as a bump or a pothole. The latter is related to continuous irregularities, such as an unpaved road. Both types impose different requirements on the suspension system that all need to be met in the design of a suspension system.

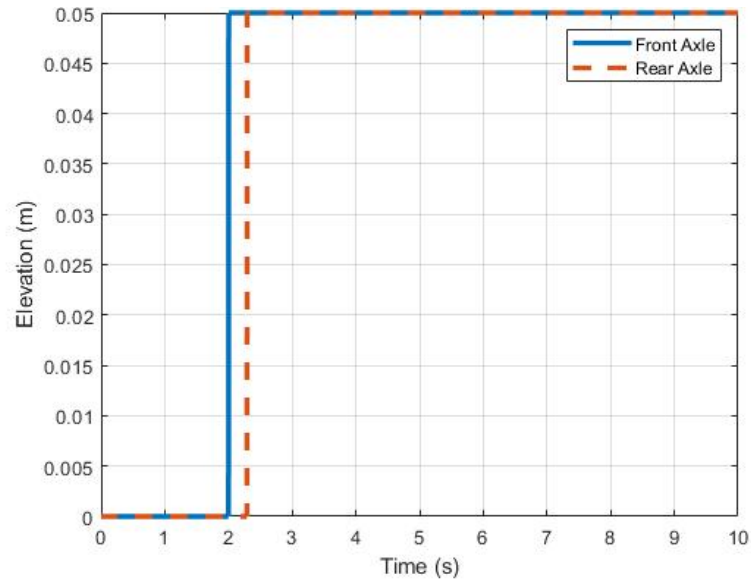
In this research, a road bump shown in Figure 5(a) and a random road profile shown in Figure 5(b) are generated. The former is illustrated in Figure 6 and its height set to $h=0.05$ m, while and its length to $L=80$ m. The vehicle velocity is constant and set to 10 m/s. In case of the full car (FC) and half car (HC1), where both front and rear axles are considered, a time lag between front and rear wheels is applied. More specifically, the front and rear wheels follow the same trajectory with a time delay $t_{distance}$, $(=(a_F+a_R)/V)$ which is due to the wheelbase. The second excitation involves a random road profile, generated based on the ISO 8608 regulation [20], which classifies road profiles according to the quality of the road. Thus, a random road profile of Class B is generated using a sinusoidal approximation. Likewise, the front and rear wheels follow the same trajectory with a time delay $t_{distance}$, which is due to the wheelbase $(a_F + a_R)$.

RESULTS

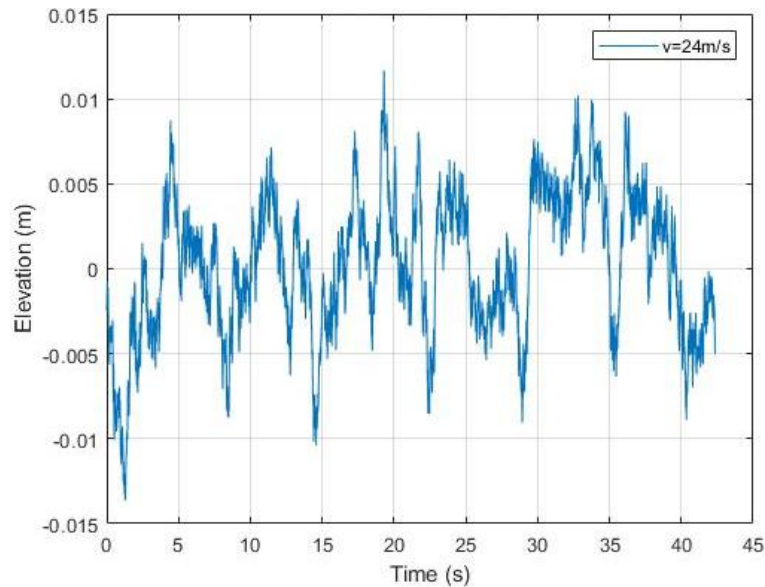
This work intends to compare the main vehicle models in terms of their accuracy. As the degrees of freedom increase and the computational cost rises, it is of significant importance to investigate not only the loss of information but also the accuracy in evaluating the performance both of the vehicle and the suspension system. Therefore, different case studies are implemented, using different suspension systems under different road excitations. Specifically, they are presented below:

- i. Part 1: In this part, all the vehicle models (QC, HC1, HC2, FC) are compared with respect to their transient and their dynamic behaviour. Firstly, they are employed with passive (Part 1a) and then with semi-active suspension system (Part 1b). In both cases, the tire damper ($c_{Ti}=0$) and the anti-roll bars ($M_{ARi}=0$) are neglected.
- ii. Part 2: In this part, the impact of additional elements in vehicle modelling is investigated. Firstly, in Part 2a two full car models are compared. The former one is the one of Part 1a, whereas the latter considers the anti-roll bars both in front and rear axle ($M_{ARi} \neq 0$). Secondly, two quarter car models are compared (Part 2b). The first one is the one of Part 1a, while the latter considers a non-zero tire damping coefficient ($c_{Ti} \neq 0$).

For each part, two types of analysis are conducted. The first type contains the analysis of transient response and in this respect the models are excited with a road bump (Figure 5a). In addition, the time-domain responses of the vehicle to the excitation are compared and the transient metrics regarding the acceleration (\ddot{z}_s) and the displacement (z_s) of the sprung mass are evaluated. Particularly for Part 2a, the transient metrics regarding the roll angle (φ) are investigated as well. Additionally, the natural frequencies (ω) of the models are calculated. The second analysis concerns the dynamic behaviour of the vehicle. In this respect the models are excited with a random road profile of class B, as illustrated in Figure 5(b), and both time-domain and frequency-domain vehicle responses are compared. Furthermore, performance metrics concerning the ride comfort, the road holding and the vehicle handling are evaluated.



(a)



(b)

Figure 5. Excitation of (a) road bump (b) random road profile based on ISO-8608.

Part 1a

In the first part, all the vehicle models (QC, HC1, HC2 and FC) are employed with passive suspension systems and are compared in terms of their accuracy. The springs of the suspension systems are considered linear, while the tire damping ($c_{Ti}=0$) and the anti-roll bars ($M_{ARi}=0$) are ignored. The vehicle parameters are selected from the literature so as to represent a passenger vehicle and are illustrated in Table 2, as used by [21]. In the following figures, the vehicle models are denoted as:

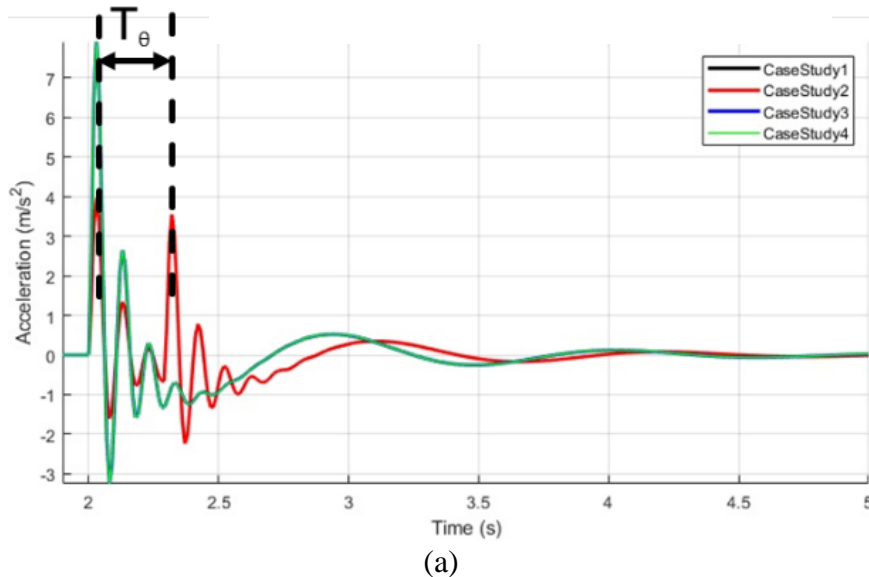
- i. Case Study 1: FC Model
- ii. Case Study 2: HC2 Model
- iii. Case Study 3: HC1 Model
- iv. Case Study 4: QC Model

Table 2. Parameters of FC model.

| Parameters | Values | Parameters | Values |
|-----------------------------------|--------|---------------------------|--------|
| m_s (kg) | 1085 | m_u (kg) | 40 |
| I_x (kgm ²) | 820 | I_y (kgm ²) | 1100 |
| a_F (m) | 1.4 | a_R (m) | 1.47 |
| b_l (m) | 0.7 | b_2 (m) | 0.75 |
| k (N/m) | 10000 | c (Ns/m) | 800 |
| k_T (N/m) | 150000 | c_T (Ns/m) | 0 |
| Additional Parameters for Part 1b | | | |
| c_{min} (Ns/m) | 400 | c_{max} (Ns/m) | 1200 |
| Additional Parameters for Part 2a | | | |
| k_R (Nm/rad) | 40000 | | |
| Additional Parameters for Part 2b | | | |
| c_T (Ns/m) | 49 | | |

Transient behaviour

As it was mentioned before, in order to evaluate the transient behaviour of the suspension systems, they are excited with a step input. The acceleration (\ddot{z}_s) and the displacement (z_s) of the sprung mass are compared in Figures 6(a) and 6(b), respectively. Additionally, in Figure 7(a) and 7(b), the acceleration (\ddot{z}_u) and the displacement (z_u) of the front right unsprung mass are illustrated. The metrics of the sprung mass acceleration are compared in Table 3, while the ones of the sprung mass displacement are shown in Table 4. In these tables the percentage of the difference of each model's metrics compared to the ones of the quarter car are evaluated ($(X-X_{QC})/X_{QC} \cdot 100\%$).



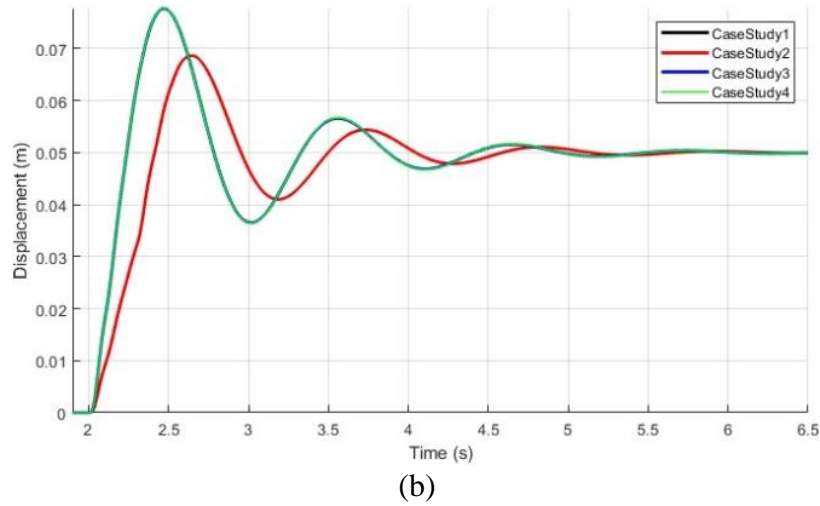


Figure 6. Part 1a - Transient behaviour: sprung mass (a) acceleration and; (b) displacement response.

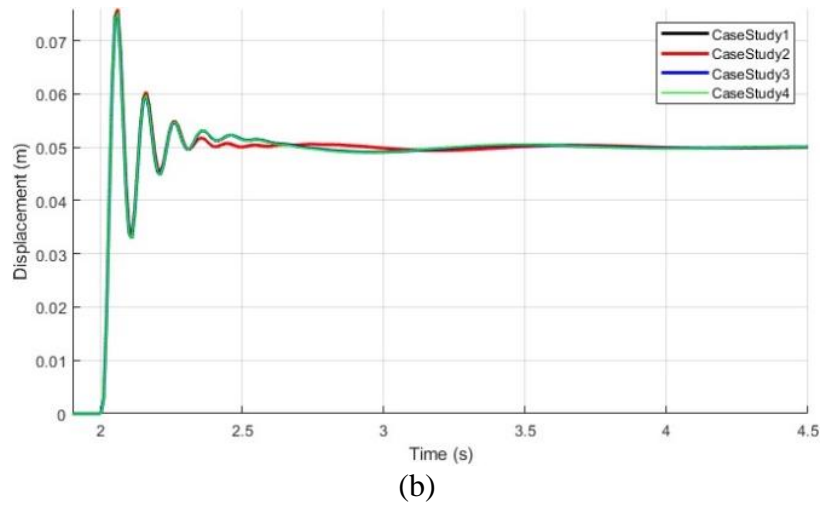
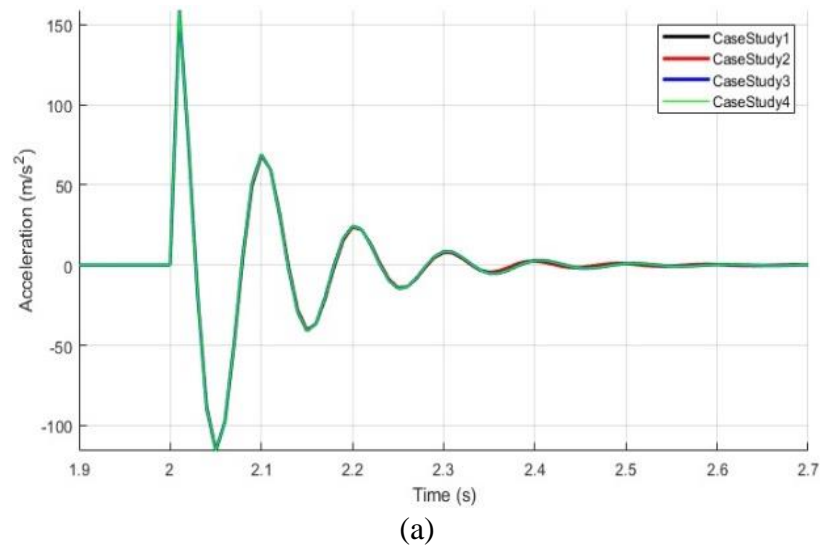


Figure 7. Part 1a - Transient behaviour: unsprung mass (a) acceleration and (b) displacement response.

Table 3. Part 1a - Transient metrics: sprung mass acceleration.

| Metrics | FC | | HC2 | | HC1 | | QC |
|---------------------------|-------|---------|-------|---------|-------|-------|-------|
| | Value | % | Value | % | Value | % | Value |
| M_p (m/s ²) | 3.97 | 49.88% | 3.97 | 49.88% | 7.92 | 0.00% | 7.92 |
| t_p (s) | 2.03 | 0.00% | 2.03 | 0.00% | 2.03 | 0.00% | 2.03 |
| t_s (s) | 4.25 | -16.58% | 4.25 | -16.58% | 3.65 | 0.00% | 3.65 |

Table 4. Part 1a - Transient metrics: sprung mass displacement.

| | FC | | HC2 | | HC1 | | QC |
|------------|-------|--------|-------|--------|-------|-------|-------|
| | Value | % | Value | % | Value | % | Value |
| M_p (mm) | 68.62 | 11.72% | 68.62 | 11.72% | 77.69 | 0.00% | 77.69 |
| t_p (s) | 2.65 | -7.29% | 2.65 | -7.29% | 2.47 | 0.00% | 2.47 |
| t_s (s) | 4.88 | -1.42% | 4.88 | -1.42% | 4.80 | 0.17% | 4.81 |

Based on the sprung mass response in Figure 6, there are two groups of waveforms that dominate. The first consists of QC and HC1 models (group 1), which present identical response, while the latter illustrates common behaviour between FC and HC2 models (group 2). The first group displays responses of greater magnitude, while all models have the same steady-state value. Additionally, according to the sprung mass acceleration response (Figure 6a) the lack of the peak that corresponds to the pitch natural frequency is noticed ($T_{\theta}=2\pi/\omega_{\theta}$). Also, the first group of models (QC and HC1) displays less damping. On the other hand, small differences between the responses of the unsprung (Figure 7) mass are noticed and they are related to the settling time of the displacement. The above remarks are confirmed by the tables of transient metrics (in Table 3 and 4). First of all, based on Table 3 and 4 the separation of the models in two groups is verified. FC and HC2 present the same percentage of difference comparing their metrics to the ones of HC1 and QC.

Table 5. Natural frequencies of vehicle models.

| | FC | HC2 | HC1 | QC |
|------------------------|-------|-------|-------|-------|
| ω_{z_s} (Hz) | 0.93 | 0.93 | 0.94 | 0.93 |
| ω_{ϕ} (Hz) | 0.78 | - | 0.78 | - |
| ω_{θ} (Hz) | 1.33 | 1.33 | - | - |
| ω_{z_i} (Hz) | 10.07 | 10.07 | 10.07 | 10.07 |

According to Table 3, the peak value of the acceleration of the QC and HC1 models increases around ~50% compared to the other two models. On the other hand, these models display more damping in the sprung mass acceleration response, with their settling time being around 16.5% lower than group 2. As far as the sprung mass displacement is concerned (Table 4), the differences between the metrics of the models are smaller. Likewise, group 1 shows greater peak value by ~12%, while its settling time is ~1.4% less. As far as the peak time variations are concerned, the second group of models has greater peaks of sprung mass displacement almost by 7.3%, in contrast to the acceleration, where no difference is noticed.

Dynamic behaviour

In order to assess the dynamic behaviour of the vehicle models, we apply as an excitation a random profile of class B. The responses of sprung mass acceleration and displacement in time-domain are compared in Figures 8(a) and 8(b), respectively, while the sprung mass acceleration response in frequency-domain is illustrated in Figure 9. Finally, the performance metrics regarding ride comfort are compared in Table 6, while the ones regarding the road holding and the vehicle handling are shown in Table 7. In these tables the percentage of the difference of each model's metrics compared to the ones of the quarter car are evaluated.

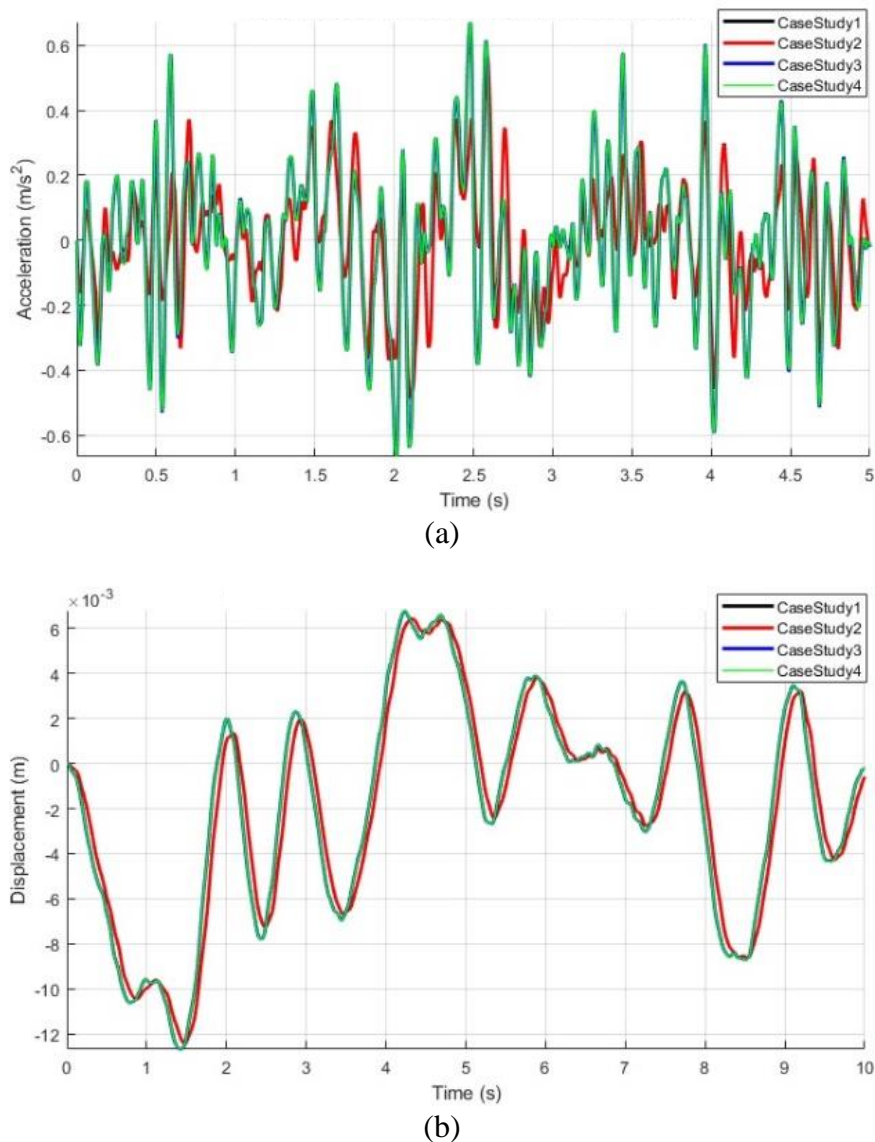


Figure 8. Part 1a - Dynamic behaviour: sprung mass (a) acceleration and; (b) displacement response in time-domain.

According to the figure, which present the time-domain responses of the sprung mass (in Figure 8), the same conclusion, as the transient analysis, is derived. As far as the frequency-domain response of the sprung mass acceleration is concerned, all models have

the same natural frequencies, while the QC and HC1 (group 1) display greater magnitudes compared to the FC and HC2 models (group 2), as shown both in Table 5 and Figure 9. As far as the ride comfort is concerned, according to the Table 6, the QC and HC1 models have greater values not only of the maximum sprung mass acceleration ($Max(\ddot{z}_s)$) but also of the weighted RMS (RC). Thus, group 1 evaluates the levels of ride comfort with less accuracy, while overestimating them.

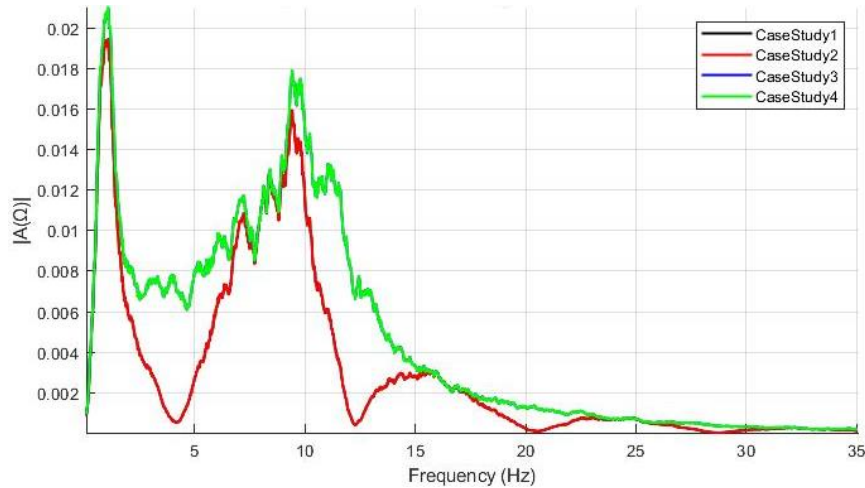


Figure 9. Part 1a - Dynamic behaviour: sprung mass acceleration response in frequency-domain.

Table 6. Part 1a - Dynamic behaviour: ride comfort metrics.

| Metrics | FC | | HC2 | | HC1 | | QC Value |
|---|-------|--------|-------|--------|-------|--------|-------------|
| | Value | % | Value | % | Value | % | |
| RC | 0.15 | 24.40% | 0.15 | 24.40% | 0.19 | 0.00% | 0.19 |
| Max(\ddot{z}_s) (m/s ²) | 0.56 | 18.40% | 0.56 | 18.40% | 0.70 | -0.59% | 0.69 |

Additionally, according to Table 7, the differences between the vehicle models are significant as far as the suspension travel is concerned. More specifically, the variances of the right and the left suspension travel of HC1 model change compared to the QC by $\sim 0.4\%$ and $\sim 0.3\%$, respectively, while the maximum values of the right and the left suspension travel differ by $\sim 1.2\%$ and $\sim 1.4\%$, respectively. The difference between the suspension travels of HC1 and the one of QC is due to the consideration of the roll angle. Considering that the right and left excitations are the same, the differences are insignificant and thus they estimate the suspension system's behaviour similarly. Furthermore, the difference noticed between FC and HC2 is less than 1% and is also due to the consideration of the roll angle and the lateral load transfer. On the other hand, as far as the comparison of FC and HC2 (group 2) with the QC is concerned, the values of the VST of group 2 regarding the front axle are by $\sim 21\%$ less, while the variances regarding the rear axle are by $\sim 14\%$ more. Accordingly, the maximum values of the suspension travel of group 2, regarding the front axle, are by $\sim 2.9\%$ less, while the maximum values regarding the rear axle are less by $\sim 7.5\%$ more. The differences between the front and rear axles is a result of including the pitch angle in the models of group 2 and the consideration of the longitudinal load transfer. Thus, the consideration of the pitch angle in a model affects the estimation regarding the behaviour of the suspension system

significantly. On the other hand, the differences in the tire deflection also exist, but they are negligible (differences less than ~1%).

Table 7. Part 1a - Dynamic behaviour: Vehicle handling and road holding metrics.

| Metrics | FC | | HC2 | | HC1 | | QC Value |
|-------------------------------------|-------|---------|-------|---------|-------|--------|----------|
| | Value | % | Value | % | Value | % | |
| VST ₁ (mm ²) | 6.22 | 20.37% | 6.16 | 21.09% | 7.77 | 0.43% | 7.81 |
| VST ₂ (mm ²) | 6.11 | 21.72% | | | 7.83 | -0.33% | |
| VST ₃ (mm ²) | 8.79 | -12.65% | 8.88 | -13.71% | 7.77 | 0.43% | |
| VST ₄ (mm ²) | 8.96 | -14.78% | | | 7.83 | -0.33% | |
| ST ₁ (mm) | 9.07 | 2.44% | 9.05 | 2.72% | 9.41 | -1.17% | 9.30 |
| ST ₂ (mm) | 9.03 | 2.94% | | | 9.17 | 1.42% | |
| ST ₃ (mm) | 9.92 | -6.73% | 9.97 | -7.19% | 9.41 | -1.17% | |
| ST ₄ (mm) | 10.01 | -7.61% | | | 9.17 | 1.42% | |
| VTD ₁ (mm ²) | 1.15 | -0.68% | 1.15 | -0.68% | 1.14 | 0.00% | 1.14 |
| VTD ₂ (mm ²) | | | | | | | |
| VTD ₃ (mm ²) | 1.13 | 0.47% | 1.13 | 0.47% | 1.14 | 0.00% | 1.14 |
| VTD ₄ (mm ²) | | | | | | | |
| TD ₁ (mm) | 4.54 | -0.97% | 4.53 | -0.93% | 4.50 | -0.08% | 4.49 |
| TD ₂ (mm) | | | | | 4.47 | 0.56% | |
| TD ₃ (mm) | 4.46 | 0.63% | 4.47 | 0.56% | 4.50 | -0.08% | |
| TD ₄ (mm) | | | | | 4.47 | 0.56% | |

Part 1b

This part investigates the vehicle models' accuracy while using semi-active suspension systems. In this respect, all the vehicle models (QC, HC1, HC2 and FC) are employed with semi-active suspension systems, operating with the SH-2 states control law, and are compared. The springs are considered linear and all anti-roll bars ($M_{ARi}=0$) as well as the tire damper ($c_{Ti}=0$) are neglected. The vehicle parameters are illustrated in Table 2. In the following figures, the vehicle models are denoted the same as before.

Transient behaviour

In Figure 10(a) and 10(b), the sprung mass acceleration (\ddot{z}_s) and displacement (z_s) responses of all models are presented, respectively. In addition, the corresponding responses (\ddot{z}_u and z_u) of the unsprung mass (front right wheel) are illustrated in Figure 11(a) and 11(b) respectively. Furthermore, the transient metrics of the sprung mass acceleration and displacement response are compared in Tables 8 and 9, respectively. In these Tables the percentage of the difference of each model's metrics compared to the ones of the quarter car are evaluated.

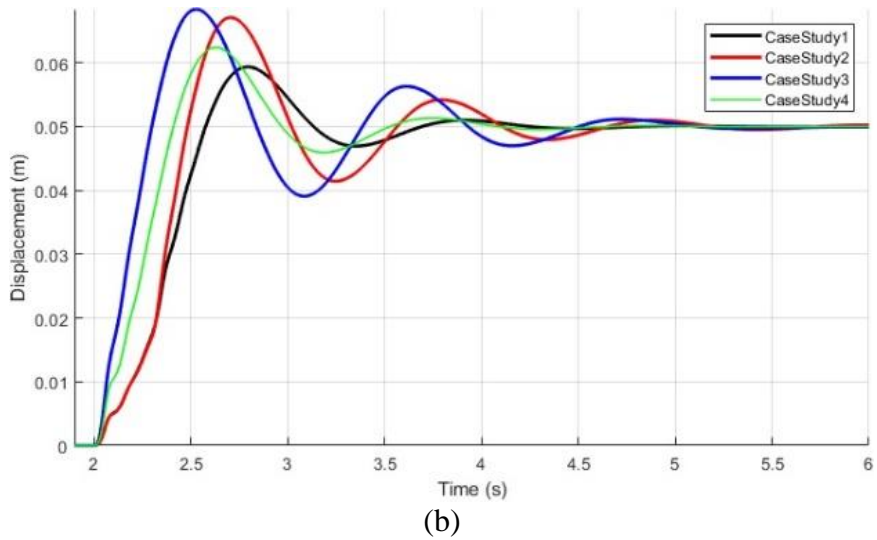
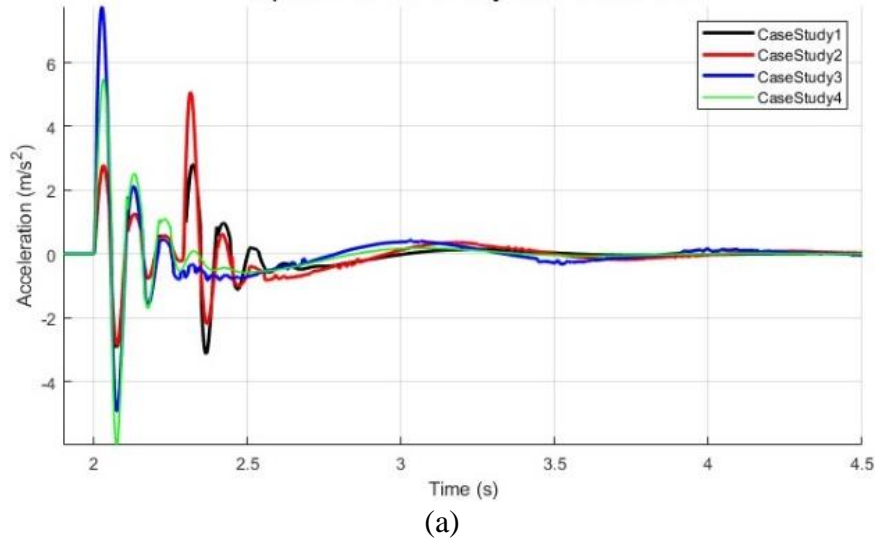
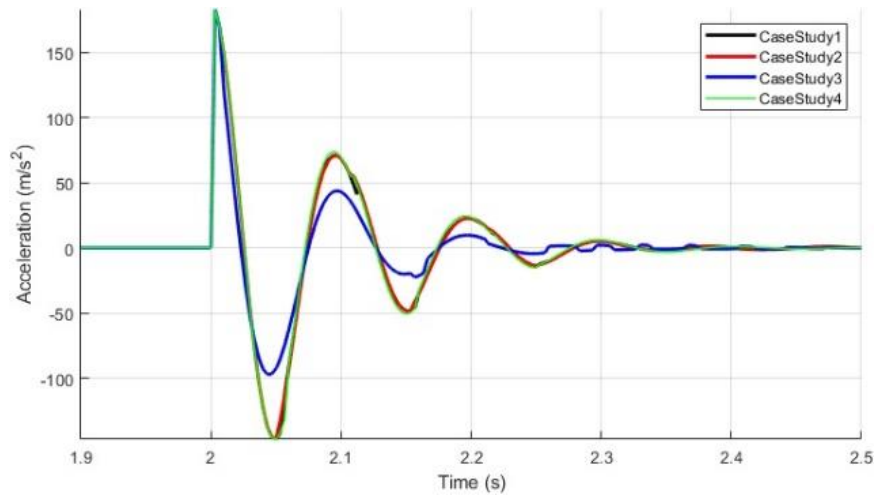


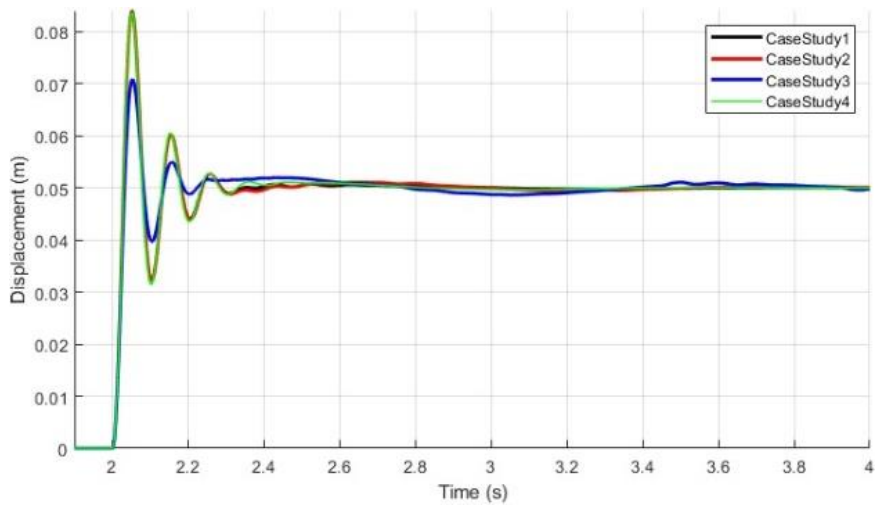
Figure 10. Part 1b - Transient Behaviour: Sprung mass (a) acceleration and (b) displacement response.

Table 8. Part 1b - Transient metrics: sprung mass acceleration.

| Metrics | FC | | HC2 | | HC1 | | QC Value |
|-------------------|-------|---------|-------|---------|-------|---------|-------------|
| | Value | % | Value | % | Value | % | |
| M_p (m/s^2) | 2.81 | 49.88% | 5.08 | 7.31% | 7.76 | -41.64% | 5.48 |
| t_p (s) | 2.32 | -14.45% | 2.31 | -13.96% | 2.03 | 0.00% | 2.03 |
| t_s (s) | 3.44 | -6.74% | 3.90 | -20.74% | 4.00 | -23.91% | 3.23 |



(a)



(b)

Figure 11. Part 1b - Transient behaviour: unsprung mass (a) acceleration and; (b) response.

According to Figure 10(a) and 10(b), all vehicle models' responses differ, regarding not only the magnitude but also the damping rate, in contrast to Part 1a, where two groups of models of similar response were identified. Specifically, Figure 10 shows that the FC model displays more damping with reduced magnitude, compared to the other models and it is less responsive. Additionally, similar with Part 1a, all models have the same steady-state value of sprung mass displacement, while the QC and HC1 models lack of the peak that corresponds to the pitch natural frequency, as shown in Figure 10(a). On the other hand, unlike Part 1a, significant differences are illustrated regarding the unsprung mass responses. More specifically, Figures 11(a) and 11(b) illustrate that the HC1 model is more oscillatory and less damped, while it displays lower magnitude, compared to the rest of the models.

The tables of transient metrics in Table 8 and 9 confirm the above remarks. More specifically, the peak value of the acceleration of the FC model is ~49% decreased compared to the QC value. As far as the peak time is concerned, both FC and HC2 models have ~14% greater value compared to the other two models, which indicates less

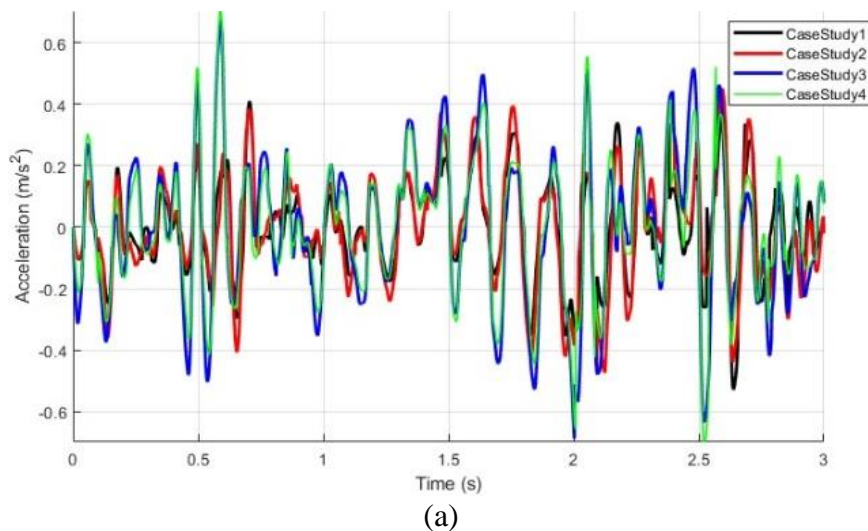
responsive behaviour. Additionally, the settling time of FC and QC models is ~20% decreased compared to the HC1 and HC2 models, and thus they settle faster. Finally, as far as the transient characteristics of the sprung mass displacement are concerned, the differences between the models are less intense, but reflect the same remarks. Likewise, the FC and HC2 models show greater peak time value (~6.2% and ~2.9%, respectively) compared to QC model, while the FC and QC models have settling time value ~25-26% less compared to HC1 and HC2 models. As far as the peak values are concerned, the value of FC is around ~5% less, while HC1 and HC2 have peak values ~7.5% and ~9.5% less compared to QC model.

Table 9. Part 1b - Transient metrics: sprung mass displacement.

| Metrics | FC | | HC2 | | HC1 | | QC |
|------------|-------|--------|-------|---------|-------|---------|-------|
| | Value | % | Value | % | Value | % | Value |
| M_p (mm) | 59.36 | 4.88% | 67.10 | -7.52% | 68.39 | -9.59% | 62.41 |
| t_p (s) | 2.79 | -6.21% | 2.71 | -2.92% | 2.53 | 3.80% | 2.63 |
| t_s (s) | 3.92 | -0.98% | 4.91 | -26.51% | 4.83 | -24.48% | 3.88 |

Dynamic behaviour

In order to assess the dynamic characteristics and the performance of the vehicle models using semi-active suspension systems, both the time-domain and frequency-domain responses are presented. Specifically, the responses of the sprung mass acceleration and the displacement in time-domain are illustrated in Figure 12(a) and 12(b) respectively. The frequency-domain response of the sprung mass acceleration is shown in Figure 13. Finally, the performance metrics regarding ride comfort are illustrated in Table 10, while the ones regarding the road holding and the vehicle handling are shown in Table 11. In these Tables, the percentage of the difference of each model's metrics compared to the ones of the quarter car are evaluated.



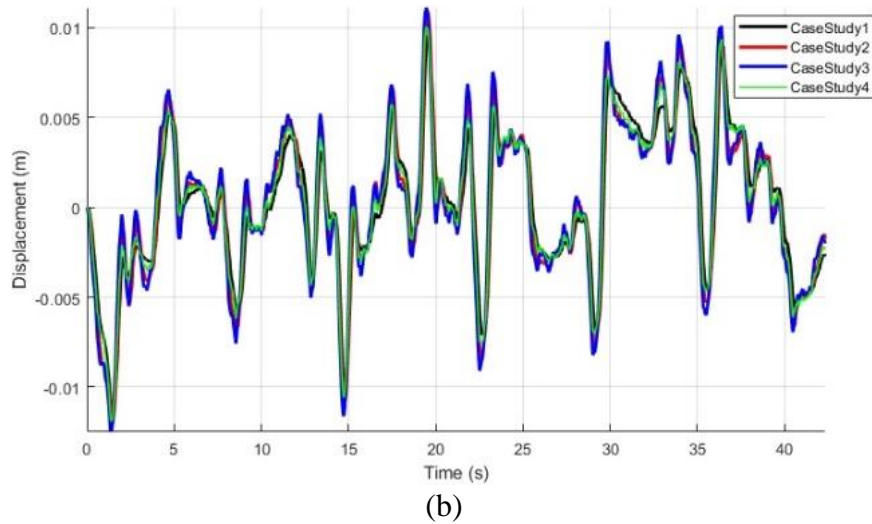


Figure 12. Part 1b - Dynamic behaviour: sprung mass (a) acceleration and (b) displacement response in time-domain.

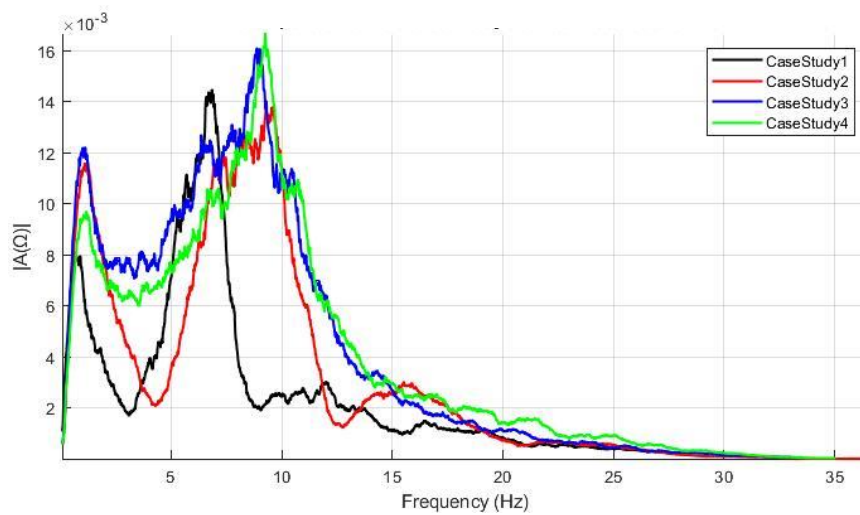


Figure 13. Part 1b - Dynamic behaviour: sprung mass acceleration in frequency-domain.

Table 10. Part 1b - Dynamic behaviour: ride comfort metrics.

| Metrics | FC | | HC2 | | HC1 | | QC Value |
|--|-------|--------|-------|--------|-------|--------|----------|
| | Value | % | Value | % | Value | % | |
| RC | 0.14 | 25.43% | 0.16 | 14.91% | 0.20 | -8.52% | 0.19 |
| Max(\ddot{z}_s)(m/s ²) | 0.65 | 18.78% | 0.60 | 25.03% | 0.76 | 5.66% | 0.80 |

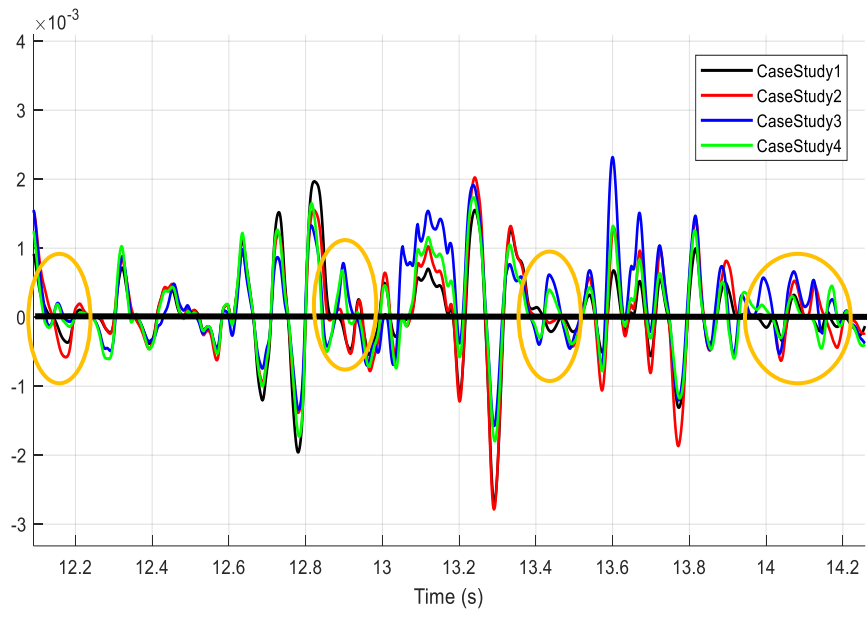
As noticed in the transient analysis, the time-domain response of the sprung mass acceleration is different for every model, regarding the magnitude, as shown in Figure 11. On the other hand, the differences between the models regarding the time-domain response of the sprung mass displacement in Figure 12(b) are insignificant, but the HC1 model displays greater magnitude similarly. Figure 13 illustrates that FC model has lower natural frequency of the unsprung mass, compared to the other models. In addition, lower

values of the magnitude of FC model's response are also noticed, while the area around 2-5 Hz of the responses of QC and HC1 models is over weighted.

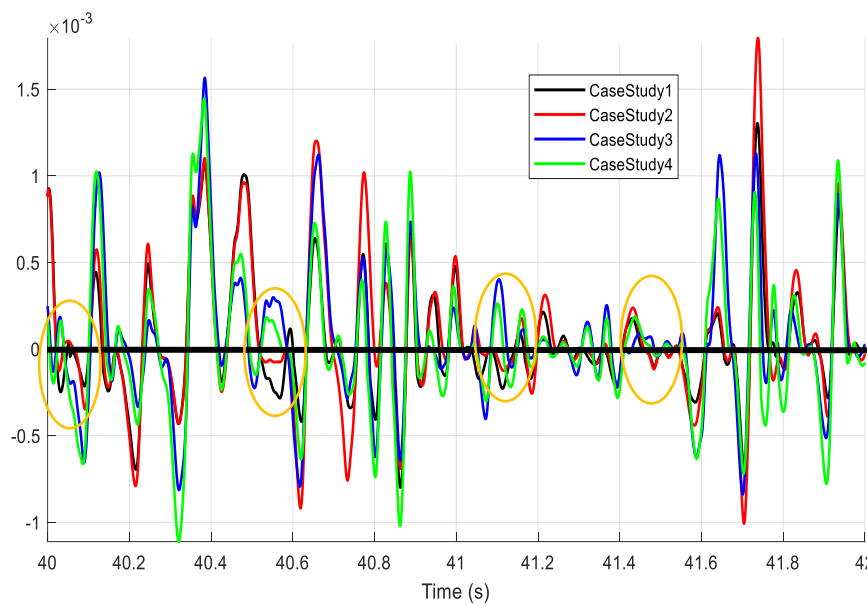
Table 11. Part 1b - Dynamic behaviour: vehicle handling and road holding metrics.

| Metrics | FC | | HC2 | | HC1 | | QC |
|-------------------------------------|-------|---------|-------|--------|-------|--------|-------|
| | Value | % | Value | % | Value | % | Value |
| VST ₁ (mm ²) | 5.13 | 10.37% | 5.65 | 1.39% | 6.20 | -8.22% | 5.73 |
| VST ₂ (mm ²) | 5.14 | 10.25% | | | 5.66 | 1.15% | |
| VST ₃ (mm ²) | 8.34 | -45.64% | 5.09 | 11.21% | 6.20 | -8.22% | |
| VST ₄ (mm ²) | 8.41 | -46.86% | | | 5.66 | 1.15% | |
| ST ₁ (mm) | 7.28 | 17.61% | 8.53 | 3.50% | 8.72 | 1.28% | 8.83 |
| ST ₂ (mm) | 7.23 | 18.11% | | | 8.50 | 3.81% | |
| ST ₃ (mm) | 10.33 | -16.88% | 7.33 | 17.04% | 8.72 | 1.28% | |
| ST ₄ (mm) | 10.36 | -17.28% | | | 8.50 | 3.81% | |
| VTD ₁ (mm ²) | 1.37 | -6.73% | 1.19 | 7.48% | 0.91 | 29.28% | 1.29 |
| VTD ₂ (mm ²) | | | | | 1.25 | 2.54% | |
| VTD ₃ (mm ²) | 1.56 | -20.87% | 0.88 | 31.38% | 0.91 | 29.28% | |
| VTD ₄ (mm ²) | | | | | 1.25 | 2.54% | |
| TD ₁ (mm) | 4.80 | 0.79% | 4.82 | 0.24% | 4.20 | 13.10% | 4.83 |
| TD ₂ (mm) | 4.79 | 0.82% | | | 4.82 | 0.24% | |
| TD ₃ (mm) | 4.83 | 0.00% | 4.12 | 14.71% | 4.20 | 13.10% | |
| TD ₄ (mm) | | | | | 4.82 | 0.24% | |

As far as the ride comfort is concerned, according to the Table 10, the FC and HC2 models have similar values of both the maximum and the RMS value of the sprung mass acceleration ($\text{Max}(\ddot{z}_s)$ and RC). Specifically, the maximum values of acceleration of the FC and BC models are by ~18.8% and ~25% less, while the RC values are by ~25.4% and ~14.91% less, compared to the QC model, respectively. These values indicate that the FC and HC2 model estimate more accurate ride comfort. Additionally, according to the Table 11, the most important difference between the models regards the suspension travel variance. More specifically, the rear suspension travel variances of the FC model have greater value compared to the QC model by ~46%. Furthermore, it is noticed that the differences between the suspension systems of each model is greater, in contrast to the Part 1a. This phenomenon is due to the semi active control law, which includes the roll and/or pitch angle in its operational conditions ($\dot{S}T$). Therefore, in few cases, the models use different state in the damper's condition under the same excitation, as displayed in Figure 14 in two different time intervals of the simulations. As a result of the above, greater variations occur in the response.



(a)



(b)

Figure 14. Part 1b - Dynamic behaviour: Control's law operational conditions of SH-2 in simulation interval between (a) 12-14 sec and; (b) 40 -42 sec.

Part 2a

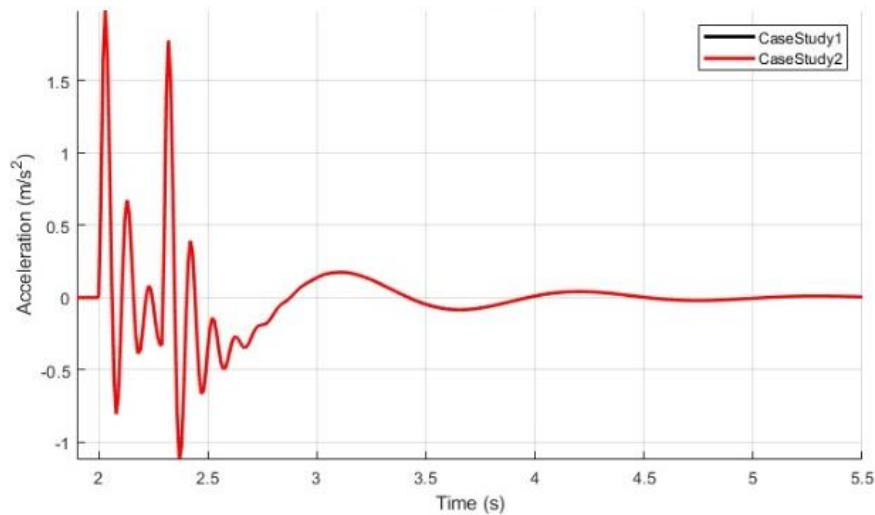
This part investigates the effect of including an anti-roll bar in the vehicle models, in terms of their accuracy. Specifically, we intent to evaluate which aspects of the vehicle's transient and steady-state responses are affected. Thus, two full car models are compared, where in the former one the anti-roll bars are neglected, while the latter includes both front and rear anti-roll bars. In both models the tire damping is neglected ($c_{Ti}=0$). In this study, the road excitation is applied only to the right side of the vehicle, in order to excite the roll plane, while investigating the vertical dynamics, and understand the importance

of considering an anti-roll bar in the vehicle model. The vehicle parameters are illustrated in Table 2. In the following figures, the vehicle models are denoted as:

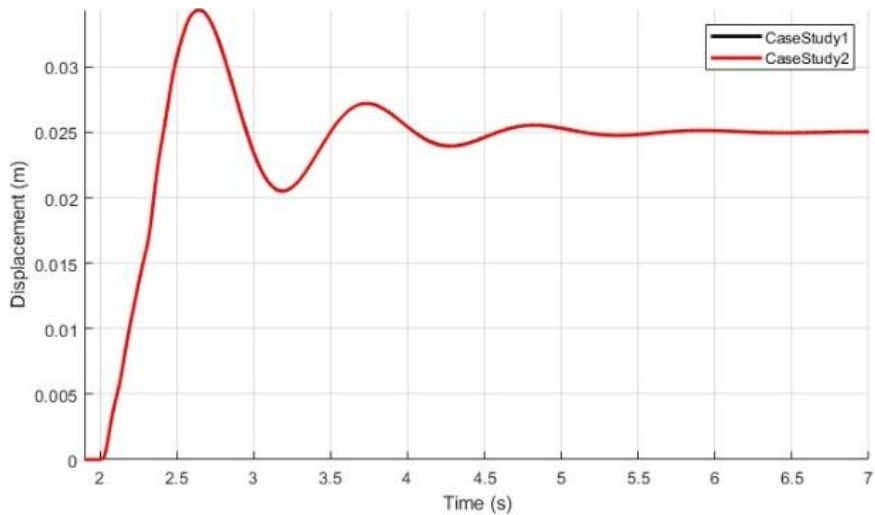
- i. Case Study 1: FC Model without anti-roll bar.
- ii. Case Study 2: FC Model with anti-roll bar.

Transient behaviour

In order to study the transient behaviour of the vehicle models, the sprung mass acceleration (\ddot{z}_s) and the displacement (z_s) are compared in the Figure 15(a) and 15(b), respectively. In Figure 16, the roll angle (ϕ) is illustrated. The transient metrics of the sprung mass acceleration and the displacement are compared in Tables 12 and 13, while the ones of the roll angle are shown in Table 14. In these tables the percentage of the differences of the metrics' values of the full car model with anti-roll bar compared to the ones of the full car model without anti-roll bar are evaluated.



(a)



(b)

Figure 15. Part 2a - Transient behaviour: sprung mass (a) acceleration and (b) displacement response.

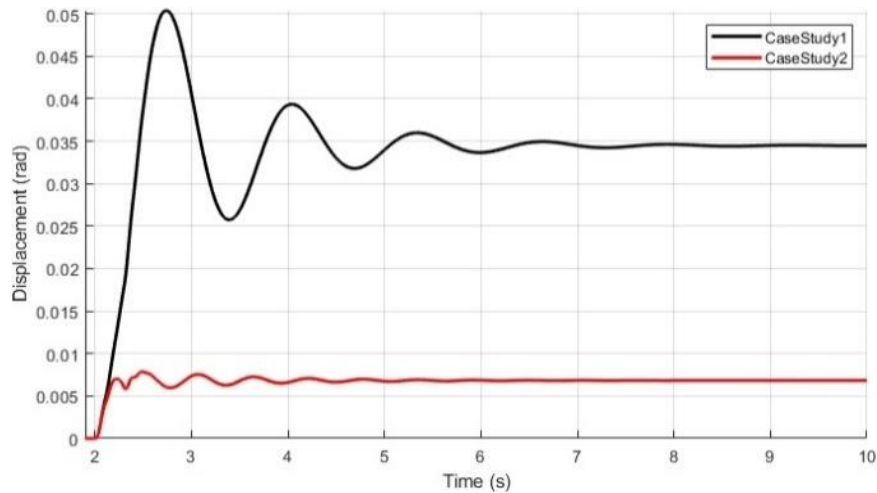


Figure 16. Part 2a - Transient behaviour: roll angle response.

Regarding the sprung mass response in Figure 15, the use of the anti-roll bar does not affect the sprung mass responses. However, Figure 16 displays a significant difference between the models, regarding both the magnitude and the damping rate. Specifically, the FC model employed with the anti-roll bars is less oscillatory and its steady-state value is less compared to the other model. The tables of transient metrics in Table 12 and 13 confirm that the use of the anti-roll bar has no impact on the sprung mass response. Additionally, Table 14 shows that the use of the anti-roll bar decreases not only the peak (~84%) and peak time (~9%) values but also the settling time (~21%) of roll angle. This indicates a more responsive and less oscillatory behaviour of the roll angle.

Table 12. Part 2a - Transient behaviour: roll angle.

| Metrics | FC with A.R. | | FC without A.R. |
|---|--------------|--------|-----------------|
| | Value | % | Value |
| M_p (rad) ($\times 10^{-2}$) | 0.79 | 84.40% | 5.04 |
| t_p (s) | 2.49 | 9.12% | 2.74 |
| t_s (s) | 4.82 | 21.08% | 6.10 |
| Steady State Value (rad) ($\times 10^{-2}$) | 0.68 | 80.29% | 3.45 |

Table 13. Part 2a - Natural frequencies.

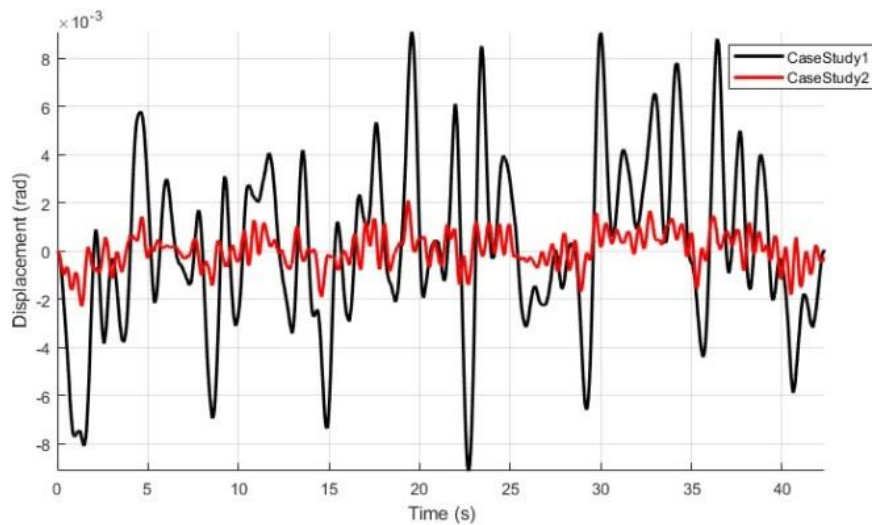
| | FC without A.R. | FC with A.R. |
|----------------------|-----------------|--------------|
| ω_{z_s} (Hz) | 0.93 | 0.93 |
| ω_ϕ (Hz) | 0.78 | 0.97 |
| ω_θ (Hz) | 1.33 | 1.33 |
| ω_{z_i} (Hz) | 10.07 | 10.07 |

According to Figure 17, the differences concerning the time-domain roll angle response are significant. As presented in the transient analysis, the use of the anti-roll bar significantly decreases the magnitude of the roll angle. As far as the frequency-domain response of the roll acceleration is concerned, Figure 18 illustrates not only the decrease of the magnitude of the response, but also the increase of the roll angle natural frequency.

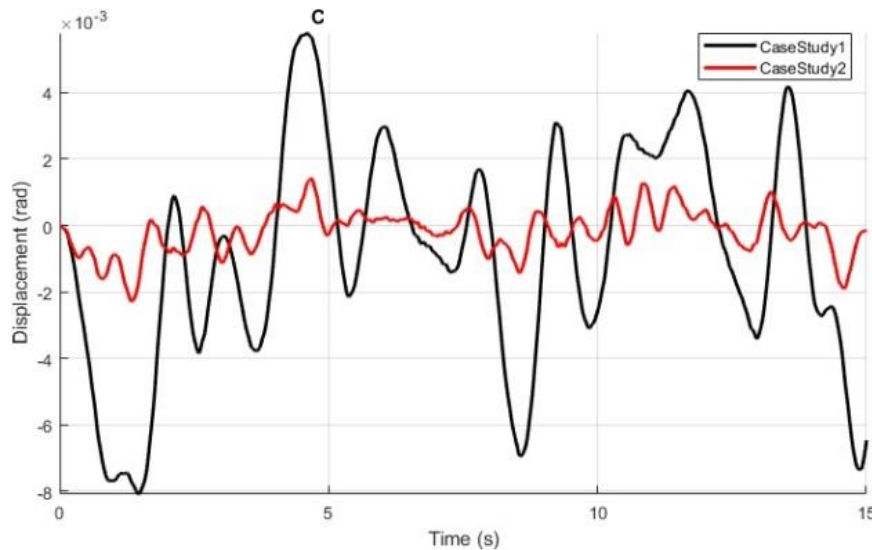
This remark is confirmed from the Table 15, which displays the natural frequencies of the models with and without the use of the anti-roll bar. Specifically, it illustrates that the roll angle natural frequency (ω_ϕ) has increased from 0.78 Hz to 0.97 Hz, while using the anti-roll bars, whereas the rest of the natural frequencies remain the same.

Table 14. Part 2a - Dynamic behaviour: ride comfort metrics.

| Metrics | FC with A.R. | | FC without A.R. |
|---|--------------|-------|-----------------|
| | Value | % | Value |
| RC | 0.07 | | 0.07 |
| Max(\ddot{z}_s) (m/s ²) | 0.27 | 0.00% | 0.27 |



(a)



(b)

Figure 17. Part 2a - Dynamic behaviour: roll angle response in time-domain. (a) complete simulation, (b) simulation interval: [0,15 s].

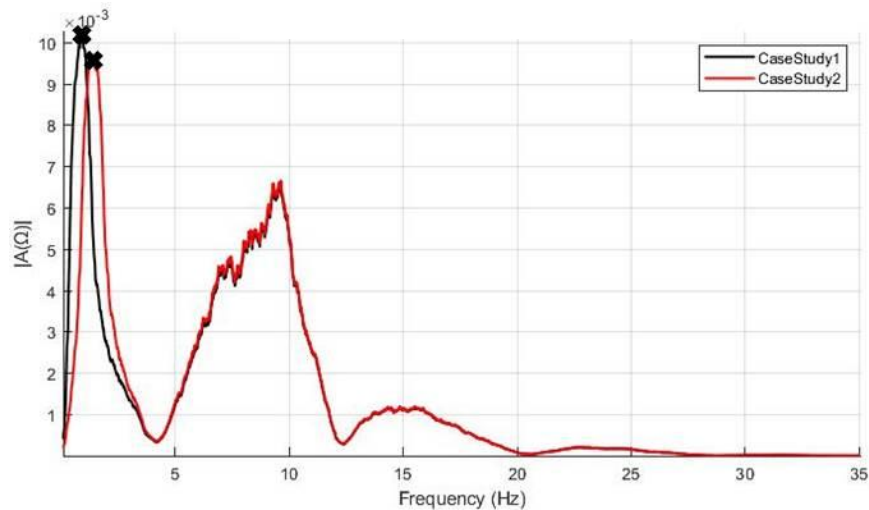


Figure 18. Part 2a - Dynamic behaviour: roll acceleration in frequency-domain.

Table 15. Part 2a - Dynamic behaviour: vehicle handling and road holding metrics.

| Metrics | FC with A.R. | | FC without A.R. |
|-------------------------------------|--------------|---------|-----------------|
| | Value | % | Value |
| VST ₁ (mm ²) | 6.28 | 1.80% | 6.40 |
| VST ₂ (mm ²) | 5.39 | -14.07% | 4.72 |
| VST ₃ (mm ²) | 7.12 | 4.18% | 7.43 |
| VST ₄ (mm ²) | 5.88 | 15.02% | 6.92 |
| ST ₁ (mm) | 7.82 | 1.21% | 7.92 |
| ST ₂ (mm) | 6.48 | -14.84% | 5.64 |
| ST ₃ (mm) | 8.43 | -0.07% | 8.42 |
| ST ₄ (mm) | 6.41 | 10.28% | 7.15 |
| VTD ₁ (mm ²) | 1.13 | 0.27% | 1.13 |
| VTD ₂ (mm ²) | 18.2 | 0.18% | 18.2 |
| VTD ₃ (mm ²) | 1.11 | 0.47% | 1.11 |
| VTD ₄ (mm ²) | 18.1 | -0.36% | 18.0 |
| TD ₁ (mm) | 4.05 | 2.25% | 4.15 |
| TD ₂ (mm) | 14.25 | -0.21% | 14.22 |
| TD ₃ (mm) | 4.06 | 2.26% | 4.15 |
| TD ₄ (mm) | 14.11 | 0.26% | 14.15 |

As far as the performance metrics are concerned, both the ride comfort (in Table 16) and the vehicle handling and road holding (in Table 17) do not display significant differences. Nevertheless, according to the Table 17, a divergence of ~10 - 15% of the variances and the maximum values of the left suspension travels is noticed (VST₂, VST₄, ST₂ and ST₄). This increase is induced since the anti-roll bar attempts to diminish the roll vibration, at the expense of the suspension travel.

Part 2b

In order to simplify and reduce the required time of the calculations, usually the tire damping is neglected. This assumption is made as the damping of tires is much smaller

than the damping of shock absorbers. In this case study, an investigation of the effect of including the tire damping in the vehicle models is conducted. In this respect, we compare two quarter car models employed with passive suspension systems, where the former has zero tire damping, while the latter considers this coefficient non-zero. The vehicle parameters are illustrated in Table 2. In the following figures, the vehicle models are denoted as:

- i. case Study 1: QC model without tire damping.
- ii. case Study 2: QC model with tire damping.

Table 16. Part 2b - Dynamic behaviour: ride comfort metrics.

| Metrics | QC with tire damper | | QC without tire damper |
|---|---------------------|-------|------------------------|
| | Value | % | Value |
| RC | 0.19 | 0.00% | 0.19 |
| Max(\ddot{z}_s) (m/s ²) | 0.67 | 3.74% | 0.69 |

Table 17. Part 2b - Dynamic behaviour: vehicle handling and road holding metrics.

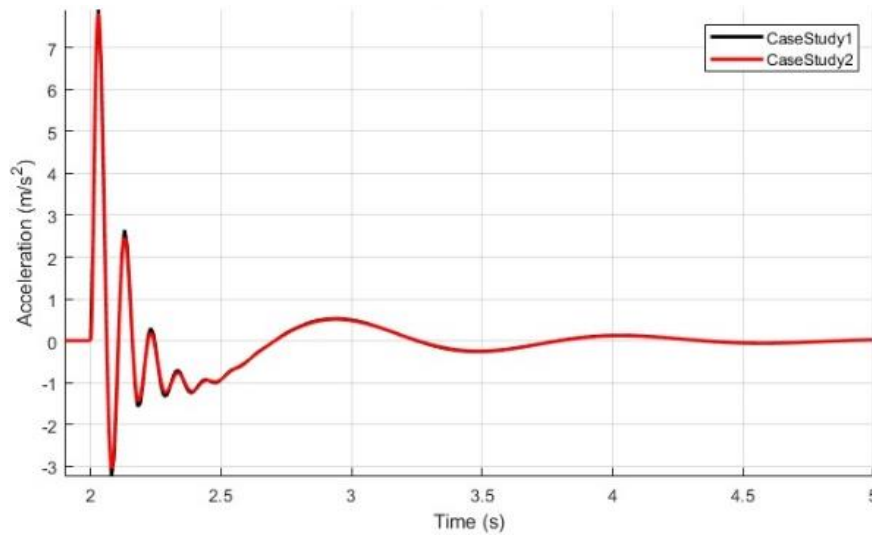
| Metrics | QC with tire damper | | QC without tire damper |
|-------------------------------------|---------------------|-------|------------------------|
| | Value | % | Value |
| VST ₁ (mm ²) | 7.74 | 0.83% | 7.81 |
| ST ₁ (mm) | 9.18 | 1.24% | 9.30 |
| VTD ₁ (mm ²) | 1.07 | 5.59% | 1.14 |
| TD ₁ (mm) | 4.42 | 1.53% | 4.49 |

Transient behaviour

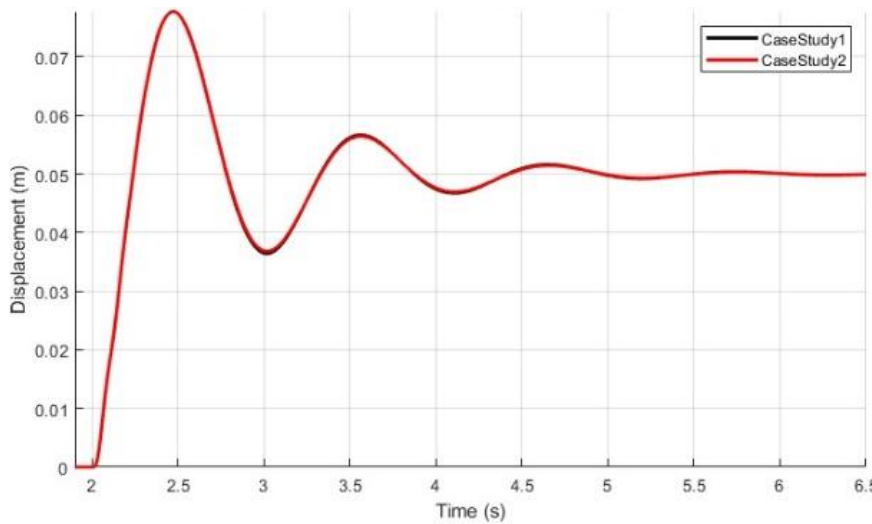
In Figure 19(a) and 19(b), the acceleration (\ddot{z}_s) and the displacement (z_s) of the sprung mass are illustrated, respectively. The transient metrics of the sprung mass acceleration and the ones of the sprung mass displacement are not displayed because of the insignificant differences. The inclusion of the tire damper in the models does not influence neither the acceleration nor the displacement. Therefore, we conclude that the assumption of zero tire damping coefficient does not affect the transient behaviour of the suspension system.

Dynamic behaviour

Considering the identical responses of Figure 19, only the response of the sprung mass acceleration in frequency-domain is illustrated in Figure 20. Also, in order to evaluate the effect of including the tire damping in the vehicle model to its dynamic characteristics, the performance metrics regarding the ride comfort are given in Table 20, while the ones regarding the road holding and the vehicle handling are shown in Table 21. In these tables the percentage of the differences of the metrics' values of the quarter car model with tire damping compared to the ones of the quarter car model without tire damping are evaluated.



(a)



(b)

Figure 19. Part 2b - Transient behaviour: sprung mass (a) acceleration and; (b) displacement response.

As far as the frequency-domain response of the sprung mass acceleration is concerned (Figure 20), the models have the same natural frequencies, while the QC model including the tire damper display a small decrease of the magnitude. According to Table 20, the models have the same weighted RMS value of acceleration (RC), but the maximum value ($Max(\ddot{z}_s)$) in the case of including the tire damper is reduced by $\sim 3.8\%$. Additionally, according to Table 21, the vehicle models have not significant differences between the values of the suspension travel as well as the maximum value of tire deflection, while the variance of the latter (VTD) in the case of including the tire damper is increased by $\sim 5.6\%$. Despite that, the models are similar in terms of vehicle handling.

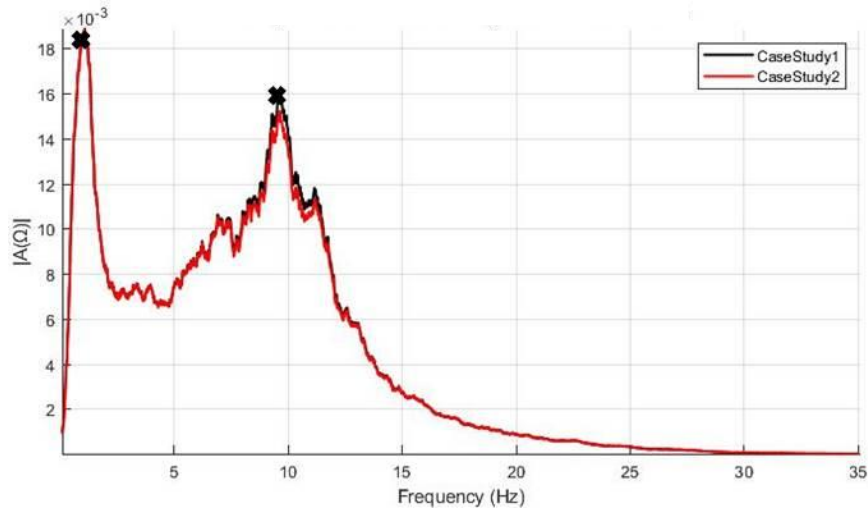


Figure 20. Part 2b - Dynamic behaviour: sprung mass acceleration in frequency-domain.

CONCLUSION

In this work, the most common vehicle models with various configurations are compared in terms of accuracy and with respect to different metrics. More specifically, both passive and semi active suspensions are considered, while the effect of adding anti-roll bars and tire dampers is investigated. The transient behaviour of the suspension system and the overall vehicle performance are assessed using different road excitations.

To sum up, in case of the models with passive suspension systems, two groups of models with identical responses occur. The first, which includes the QC and HC1 models, estimates vehicle's behaviour with less accuracy than the latter group, which consists of the HC2 and FC models. The differences between the models of each group are negligible, therefore the higher accuracy models are not necessary to be used. However, the higher accuracy models should be used only if different excitation are intended to be applied, which will trigger the roll dynamics. This remark could save significant computational time from the suspension design engineers in Research and Industry and specifically when optimisation procedures are applied, which are extremely demanding. Moreover, in the case of employing the models with semi-active suspension systems, all the models display different responses to the excitation without illustrating a similar trend likewise the passive suspensions. This is because both pitch and roll angle are included in the operational conditions of the control law studied when the model considers them as DoFs. Therefore, the operational conditions differ significantly between the vehicle models and in few cases, the dampers use different state in their conditions. Therefore, in vehicle models with control laws that include the roll angle or the pitch angle, the loss of information may be greater if QC is used for example instead of HC or FC.

As far as the additional elements are concerned, the use of the anti-roll bar affects only the roll response, increasing the natural frequency, decreasing the magnitude and affecting the transient characteristics of the roll angle. However, the consideration of the anti-roll in the vehicle doesn't affect the metrics depicting the ride comfort of the passengers. Therefore, in such cases where the attention is turned on ride comfort, we may neglect the anti-roll bars without costing accuracy in our results. Last but not least, the consideration of the tire damper in the models has no significant impact to neither the transient nor the dynamic behaviour of the models, and thus the assumption of zero

damping does not affect the accuracy of the models, validating the proposal of researcher to neglect it.

REFERENCES

- [1] Barethiye VM, Pohit G, Mitra A. Analysis of a quarter car suspension system based on nonlinear shock absorber damping models. *International Journal of Automotive and Mechanical Engineering*; 14. Epub ahead of print 2017.
- [2] Koulocheris D, Papaioannou G. Dynamic analysis of the suspension system of a heavy vehicle through experimental and simulation procedure. In: 25th JUMV International Automotive Conference “Science and Motor Vehicles”. 2015, pp. 187–199.
- [3] Ramamurthy J, Choi S-B. A novel semi-active control strategy based on the cascade quantitative feedback theory for a vehicle suspension system. *Proceedings of the Institution of Mechanical Engineers, Part D: Journal of Automobile Engineering* 2018; 1–13.
- [4] Koulocheris D, Papaioannou G. Experimental evaluation of the vertical wheel loads of a heavy vehicle validated with an optimized half car model. In: 11th HSTAM International Congress on Mechanics. 2016, pp. 27–30.
- [5] Papaioannou G, Koulocheris D. An approach for minimizing the number of objective functions in the optimization of vehicle suspension systems. *Journal of Sound and Vibration* 2018; 435: 149–169.
- [6] Papaioannou G, Koulocheris D. Optimization of skyhook control strategies and an alternative approach for the operational conditions. 2018.
- [7] Koulocheris D, Papaioannou G, Chrysos E. A comparison of optimal semi-active suspension systems regarding vehicle ride comfort. *IOP Conference Series: Materials Science and Engineering*; 252. Epub ahead of print 2017.
- [8] Koulocheris D, Papaioannou G, Christodoulou D. An approach for multi-objective optimization of vehicle suspension system. *IOP Conference Series: Materials Science and Engineering*; 252. Epub ahead of print 2017.
- [9] Fossati GG, Miguel LFF, Casas WJP. Multi-objective optimization of the suspension system parameters of a full vehicle model. *Optimization and Engineering* 2018; 20: 151–177.
- [10] Abdelkareem MAA, Xu L, Guo X, et al. Energy harvesting sensitivity analysis and assessment of the potential power and full car dynamics for different road modes. *Mechanical Systems and Signal Processing* 2018; 110: 307–332.
- [11] Seifi A, Hassannejad R, Hamed MA. Optimum design for passive suspension system of a vehicle to prevent rollover and improve ride comfort under random road excitations. *Proceedings of the Institution of Mechanical Engineers, Part K: Journal of Multi-body Dynamics* 2016; 230: 426–441.
- [12] Shim T, Velusamy PC. Improvement of vehicle roll stability by varying suspension properties. *Vehicle System Dynamics* 2011; 49: 129–152.
- [13] Tchamna R, Youn E, Youn I. Combined control effects of brake and active suspension control on the global safety of a full-car nonlinear model Combined control effects of brake and active suspension control on the global safety of a full-car nonlinear model. *Vehicle System Dynamics* 2014; 52: 69–91.
- [14] Cao D, Rakheja S, Su CY. Roll- and pitch-plane-coupled hydro-pneumatic suspension. Part 2: Dynamic response analyses. *Vehicle System Dynamics* 2010; 48(4), 507-528.

- [15] Faris WF, Ihsan SI, Ahmadian M. Transient and steady state dynamic analysis of passive and semi-active suspension systems using half-car model. *International Journal of Modelling, Identification and Control* 2009; 6: 62.
- [16] Ihsan SI, Faris WF, Ahmadian M. Dynamics and control policies analysis of semi-active suspension systems using a full-car model. *International Journal of Vehicle Noise and Vibration* 2007; 3: 370–405.
- [17] Ihsan SI, Faris WF, Ahmadian M. Analysis of control policies and dynamic response of a Q-car 2-DOF semi active system. *Shock and Vibration* 2008; 15: 573–582.
- [18] Faris WF, BenLahcene Z, Hasbullah F. Ride quality of passenger cars: an overview on the research trends. *International Journal of Vehicle Noise and Vibration* 2012; 8: 185.
- [19] International Organization for Standardization. Mechanical vibration and shock-Evaluation of human exposure to whole-body vibration - Part 1 : General requirements, ISO 2631-1 : 1997, 1997. 1997.
- [20] International Organization for Standardization. Mechanical vibration-Road surface profiles-Reporting of measured data. 1995.
- [21] Jazar RN. *Vehicle dynamics : Theory and application*. 3rd ed. Cham: Springer, 2014. Epub ahead of print 2014.